

Nonlinear Seismic Analysis of Perforated Steel Plate Shear Walls



A.K. Bhowmick

Concordia University, Canada

G.Y. Grondin & R.G. Driver

University of Alberta, Canada

SUMMARY:

The behaviour of unstiffened steel plate shear walls with circular perforations in the infill plate was examined. A shear strength model is developed based on a strip model where all the strips with perforations are discounted. Eight perforation patterns in single storey steel plate shear walls of two different aspect ratios were analyzed using a non-linear finite element model to assess the proposed shear strength model. A comparison between the non-linear pushover analysis and the proposed equation shows excellent agreement. The proposed shear strength model for perforated shear walls is applied for design of boundary columns of one 4-storey shear wall. The predicted design forces (axial forces and bending moments) in the boundary columns for the 4-storey perforated shear wall are compared to the forces obtained from nonlinear seismic analysis. The proposed model gives excellent predictions for the design forces in the columns.

Keywords: Steel Plate Shear Wall, Seismic analysis, Circular perforations

1. INTRODUCTION

The steel plate shear wall (SPSWs) is a very effective system for resisting lateral loads due to wind and earthquakes. A properly designed SPSW has high ductility, high initial stiffness, high redundancy, and excellent energy absorption capacity. Current North American practice consists of using thin unstiffened plates for the infill plates, relying on tension field action to provide high lateral resistance.

Very often, the infill plate used in a SPSW is thicker and stronger than required by the design. In fact, handling and welding considerations are likely to govern the selection of the thickness of the infill plate in the majority of cases. Increasing the plate thickness to suit fabrication considerations often introduces a problem in capacity design, as this will introduce excessive design forces to the surrounding frame members, thus increasing their required size. Recent attempts to address this problem have included the use of light-gauge, cold-formed, steel infill plates or low yield strength steel for infill plates (Berman and Bruneau 2005, Vian 2005), introducing vertical slits in the infill plate (Hitaka and Matsui 2003, Cortes and Liu 2011), or by introducing a regular pattern of circular perforations in the infill plate (Vian 2005). Among all the proposed options, the perforated SPSW recommended by Vian (2005) represents an attractive system since it also provides a route for the utility systems to pass through the infill plates.

Research on circular perforations in shear panels similar to SPSWs started with Roberts and Sabouri-Ghomi (1992). They conducted a series of cyclic loading tests on unstiffened steel plate shear panels with centrally-placed circular openings. Based on the test results, the researchers proposed the following approximate equation for the strength of an unstiffened infill panel with a central circular opening:

$$V_{op} = V_p \left(1 - \frac{D}{d_p} \right) \quad (1.1)$$

where V_{op} and V_p are the strength of a perforated and a solid shear panel, respectively, D is the perforation diameter, and d_p is the panel height.

Purba (2006) analyzed a 4000x 2000 mm single storey SPSW with multiple regularly-spaced circular perforations of equal diameter. The effects of infill plate thickness and perforation diameter were considered in the analysis. It was observed that for multiple regularly spaced perforations, Eq. (1.1) provides a conservative estimate of the strength of the perforated infill plate when d_p is replaced by S_{diag} , the diagonal distance between each line of perforations. Through a calibration study, the following modified equation was proposed to calculate the shear strength of perforated SPSWs with the regular perforation pattern used by Vian (2005):

$$V_{op} = V_p \left(1 - 0.7 \frac{D}{S_{diag}} \right) \quad (1.2)$$

Purba (2006) also found that results from an individual perforated strip analysis can accurately predict the behaviour of a complete perforated SPSW provided that the hole diameter is less than 60% of the strip width $\left(\frac{D}{S_{diag}} \leq 0.6 \right)$. Although Eq. (1.2) was found to provide good strength predictions of SPSWs for the regular perforation pattern proposed by Vian (2005), a more general expression, applicable to any pattern of perforations, is clearly desirable.

This paper presents a general equation for determining the strength of perforated SPSWs. The proposed equation is based on a strip model, and is derived by discounting the strips that are intercepted by perforations. Finite element models of two single storey SPSWs (with aspect ratios of 2.0 and 1.5) and with eight different types of perforation patterns are analyzed to investigate the effectiveness of the proposed equation.

AISC Steel Design Guide 20 (Sabelli and Bruneau 2007) presents a capacity design method for the design of SPSW columns with solid infill plates. The method in AISC Steel Design Guide 20 (Sabelli and Bruneau 2007) assumes that the infill plates over the entire building height reach their full yield capacity, and plastic hinges are assumed at the ends of all the horizontal members of the frame. Forces from the infill plate tension fields and the force effects from the beams are then applied to a free body diagram of the boundary columns to determine their design axial forces and moments. The presence of perforations in the infill plates affects the forces and moments in the boundary columns, thus requiring modifications to the current design method.

This paper proposes modifications to the capacity design method of AISC Steel Design Guide 20 (Sabelli and Bruneau 2007) to accommodate SPSWs with circular perforations. The modified capacity design method is used to design the columns of one 4-storey SPSW with four circular perforations. The resulting design forces for the boundary columns are compared with the design forces obtained from a seismic analysis of the 4-storey SPSW under four spectrum-compatible earthquake ground motions for Vancouver, Canada.

2. STRENGTH EQUATION FOR PERFORATED INFILL PLATE

To develop a general strength model, it is assumed that the infill plate has negligible buckling capacity and that the shear strength of the SPSW is provided strictly by tension field action. The angle of inclination of the tension field, α , is obtained from the equation specified in the Canadian standard, CAN/CSA S16-09 (CSA 2009), and in the AISC seismic Specification (AISC 2005). In the presence of a circular hole of diameter D , as shown in Fig. 2.1, one can discount part of the contribution, β , of the steel within a diagonal strip of width D (Vian 2005). Therefore, it is assumed that only a portion

of that tension strip with an equivalent width $D(1 - \beta)$ will be effective. Taking the diagonal strip containing the circular hole to be at the angle of the tension field, α , the horizontal projection of the portion of the strip to be discounted is $\beta \frac{D}{\cos \alpha}$. After discounting the strip with the circular perforation, the effective width of the infill plate, $L_{p,eff}$, becomes:

$$L_{p,eff} = L_p - \beta \frac{D}{\cos \alpha} \quad (2.1)$$

where L_p is the width of perforated infill plate.

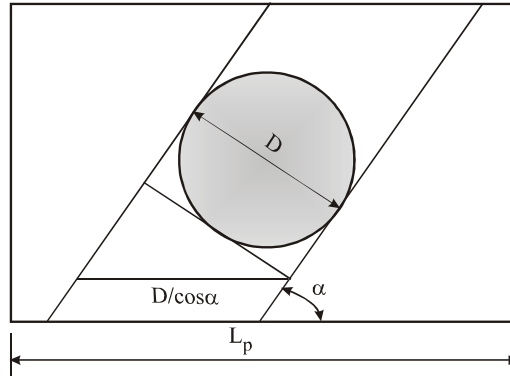


Figure 2.1. Strip model for perforated infill plate

When more than one strip is perforated and all the strips around the circular perforations are parallel and inclined at an angle α , the effective width of the perforated infill plate, $L_{p,eff}$, is

$$L_{p,eff} = \left(L_p - N_r \beta \frac{D}{\cos \alpha} \right) \quad (2.2)$$

where N_r is the maximum number of diagonal strips (at any section, cut parallel to length L_p , over the height of the panel) with circular perforations to be discounted.

Thus, the shear strength of a perforated infill plate, V_{op} is

$$V_{op} = 0.5 \sigma w \left(L_p - N_r \beta \frac{D}{\cos \alpha} \right) \sin 2\alpha \quad (2.3)$$

where w is the infill plate thickness and σ is the stress in the infill plate (remaining solid) tension strips, taken as the yield stress for design.

The shear strength of a solid infill plate, V_p , is given by

$$V_p = 0.5 \sigma w L_p \sin 2\alpha \quad (2.4)$$

From Eqs. (2.3) and (2.4)

$$\frac{V_{op}}{V_p} = \left(1 - \beta N_r \frac{D}{L_p \cos \alpha} \right) \quad (2.5)$$

As discussed in the next section, the value of the constant β is obtained from the analysis of a series of one-storey SPSWs with a variety of perforation patterns.

3. ANALYSIS OF PERFORATED STEEL PLATE SHEAR WALLS

Nonlinear finite element analyses of a series of single-storey SPSWs were carried out using the general purpose finite element analysis software ABAQUS (Hibbitt et al., 2007) to determine the magnitude of the constant β . Both material and geometric nonlinearities were considered. In total, eight different types of perforation patterns were considered in this study. Variation in perforation diameter was also considered for each type of perforation pattern.

3.1. Selection of the shear wall system

The single-storey SPSW considered here is a part of a hypothetical symmetrical office building located in Vancouver, Canada. The building has a total area of 2014 m² and a height of 3.8 m. The building has two identical SPSWs to resist lateral loads in each direction. For simplicity, torsional effects are neglected. Therefore, each shear wall was assumed to resist one half of the design seismic loads. Each shear wall is 7.6 m wide, measured from centre to centre of columns. The building was assumed to be on rock (site class B according to NBCC 2005). A dead load of 1.12 kPa was used for the roof. The snow load at the roof was taken as 1.48 kPa. Design seismic load was calculated using the equivalent static force procedure of the National Building Code of Canada, NBCC 2005 (NRCC 2005). As prescribed by NBCC 2005, a ductility-related force modification factor, R_d , of 5.0 and an overstrength force modification factor, R_o , of 1.6 were used in the design. An infill plate thickness of 3.0 mm was used. The value of the angle of the diagonal tension field was taken as 45°. With the angle of the tension field known, boundary beams and columns were selected. For the top and bottom beams, a W610x498 section was selected to anchor the tension forces from the yielded infill plate. W360x900 columns were selected to carry the forces developed in the yielded infill plate and the plastic hinges at the ends of the top beam. Figure 3.1 shows the eight different perforation patterns used in this investigation. The perforations are placed in such a way so that the SPSW behaviour remains symmetrical under the lateral loads applied from both directions. The figures also show that strips are drawn at 45° around the perforations. All the circular perforations shown in Fig. 3.1 have a diameter of 500 mm.

3.2. Characteristics of the finite element model

The infill plate and boundary members (beams and columns) were modeled using a general purpose four-node, doubly-curved, shell element with reduced integration (ABAQUS element S4R). The beams and columns were rigidly connected together and the infill plate was connected directly to the beams and columns. Initial imperfections were applied in the model to help initiate buckling in the infill plate and the development of the tension field. The infill plate was taken to have an initial imperfection pattern corresponding to the first buckling mode of the plate wall with a peak amplitude of 1 mm. Thus, an eigenvalue buckling analysis was first run on the perfect SPSW (with a flat infill plate) to extract the first buckling mode.

The modulus of elasticity was taken as 200 000 MPa. An elasto-plastic stress versus strain curve was adopted, with a yield strength of 385 MPa for the infill plates, and 350 MPa for the beams and columns. A displacement control solution strategy where the top storey displacement was used as the control parameter was used in this work. A target displacement of 110 mm was selected for all the pushover analyses of the single storey SPSWs.

3.3 Pushover analysis

SPSWs with the eight different perforation patterns shown in Fig. 3.1 were modeled and analyzed. A reference SPSW with a solid infill plate was also analyzed to compare the behaviour with perforated SPSWs. It may be more rational, instead of comparing the total shear strengths, which include both the strength of the infill plate and that of the boundary frame, to compare only the infill plate strengths with different perforation patterns. Thus, a model consisting of only the rigid frame of the SPSW was

also analyzed. Shear strengths of 9771 kN and 6269 kN were obtained for the single storey SPSW with the solid infill plate and without any infill plate (bare frame), respectively.

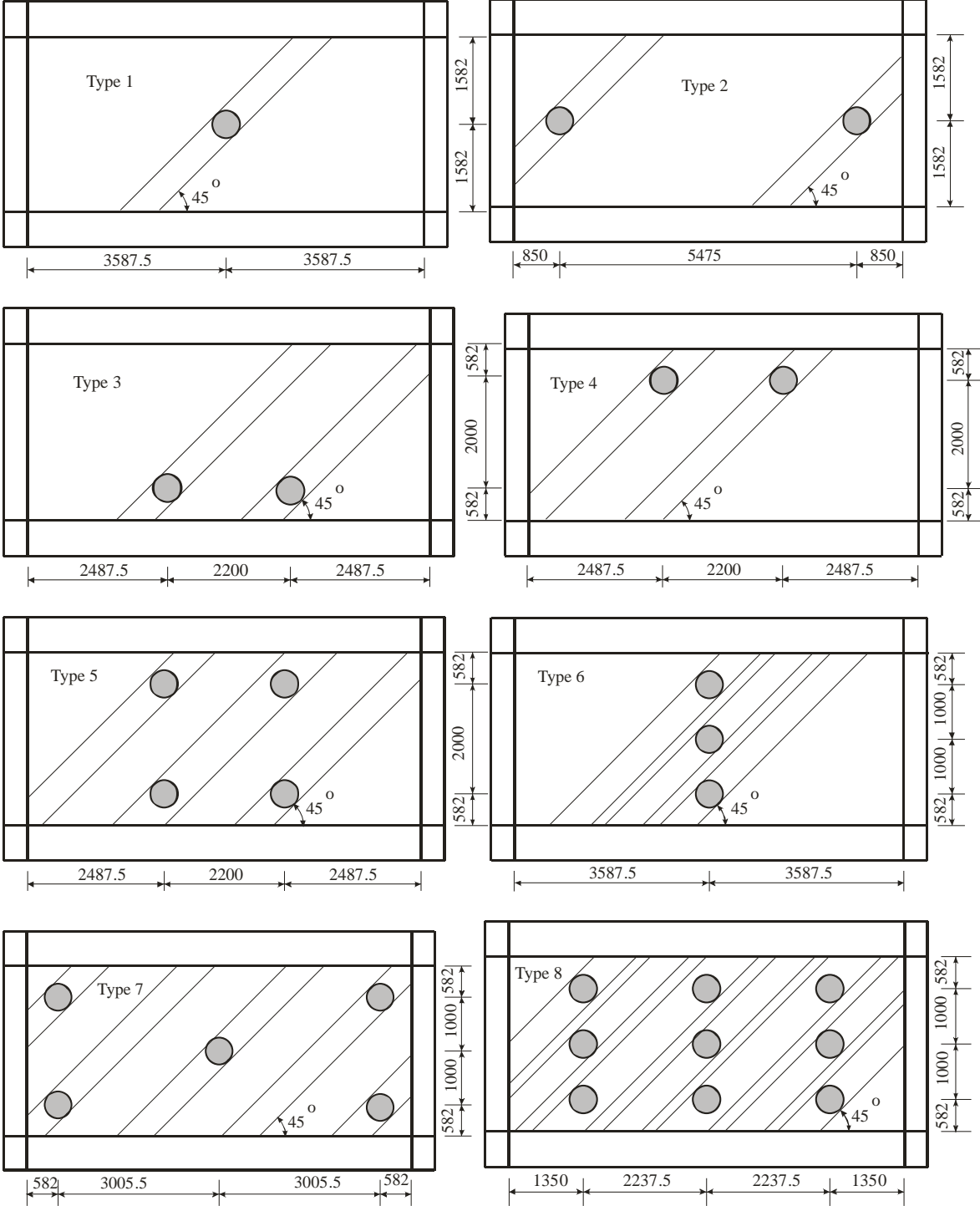


Figure 3.1. Selected perforation layouts

To examine the effect of perforation diameter, all eight perforation patterns illustrated in Fig. 3.1 were re-analyzed for two other perforation diameters, namely, 400 mm and 600 mm. The cases designated Type 2, Type 3 and Type 4 have only two circular perforations at different locations, and therefore two strips can be discounted. Also, for Type 5 and Type 8 arrangement of perforations, about 3.3 and 7.6 equivalent strips are discounted. Since for Type 8 perforation pattern, maximum numbers of strips

are discounted (in this study), for all three perforation diameters, the Type 8 case resists a lower base shear than any other perforation type considered here. Figure 3.2 shows the deformed mesh for the Type 5 perforation case. The grey patches in this plot represent complete yielding. It can be observed that a significant portion of the diagonal strips along the perforations is not yielded and thus can be discounted.

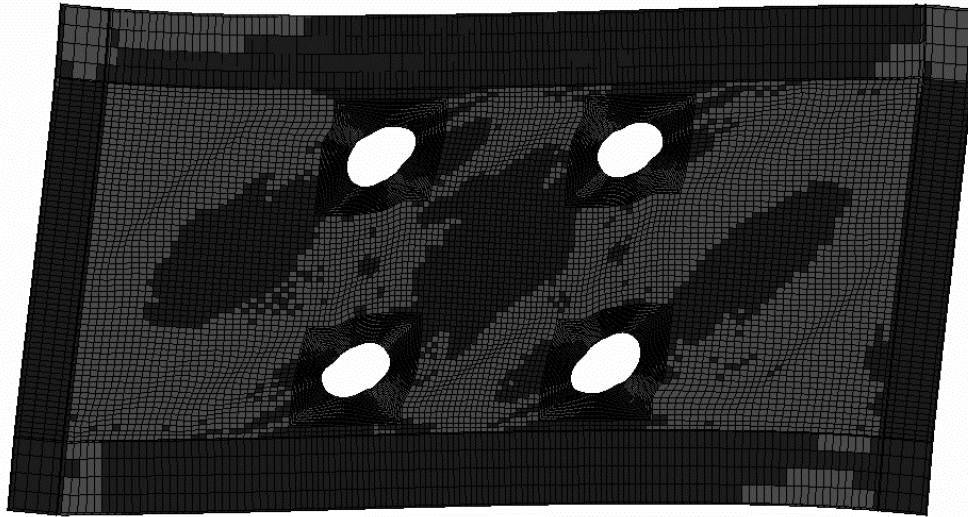


Figure 3.2. Deformed FE mesh for Type 5 perforation

By assuming the overall SPSW strength can be approximated by the summation of the base frame and the infill plate strengths, it is possible to estimate the infill plate strength by subtracting the bare frame strength from the total strength at the same displacement level, namely, 110 mm, as selected here. Thus, ratios of perforated infill plate strengths to the solid infill plate strength, V_{op}/V_p , were calculated for all perforation configurations. The ratios of V_{op}/V_p for the three different perforation diameters were then used in Eq. (2.5) to evaluate the constant β . Estimated values of β for the 24 cases considered are plotted against V_{op}/V_p in Fig. 3.3. Except for the wall with a single perforation, Type 1 (where β ranges from 1.3 to 1.4), it was observed that the β values are very similar. For Type 1 cases, it was observed from pushover analysis that more than the one strip containing the hole was discounted, which is contrary to all the other cases. To further investigate the effect of placing a single perforation in the infill plate, Type 2 and Type 3 cases with a hole diameter of 400 mm were re-analyzed with only one perforation (the left perforation for Type 2 and Type 3). The ratios of V_{op}/V_p for these two cases were the same, 0.93, which gives a value of β equal to 0.88. Thus, for 400 mm perforation, the shear strength of the infill plate reduced more when the single perforation is placed at the center of the infill plate (4.3% for the cases studied). Nevertheless, since there is only one hole, unless it is very large the increased impact on the overall wall capacity is relatively small. The mean of all β values in Fig. 3.3, excluding the three values obtained for a single perforation at the center, is 0.69. A value of 0.7 was selected for the constant β in Eq. (2.5).

The proposed equation (Eq. (2.5)) with the value of $\beta = 0.7$ was used for the prediction of the reduction in shear strength for a SPSW with an aspect ratio of 1.5 (SPSW width of 5.7 m). Again, an infill plate thickness of 3.0 mm was used. In this case, a W530x272 section was selected for the top and bottom beams and a column section of W360x509 was selected to carry the forces developed from infill plate yielding and plastic hinging at the ends of the top beam. Similar eight perforation patterns, as analyzed for an aspect ratio 2.0, were also considered for the SPSWs with an aspect ratio of 1.5.

Nonlinear pushover analyses of all eight perforation patterns were carried out for a storey displacement of 110 mm. Ratios of perforated infill plate strengths to the solid infill plate strength, V_{op}/V_p , were calculated and are compared with the values obtained from Eq. (2.5) in Fig. 3.4. Excellent agreement is observed between the finite element analysis results and Eq. (2.5).

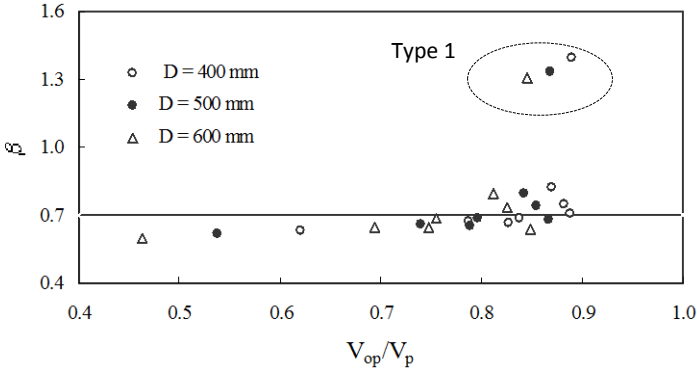


Figure 3.3. Estimation of constant β

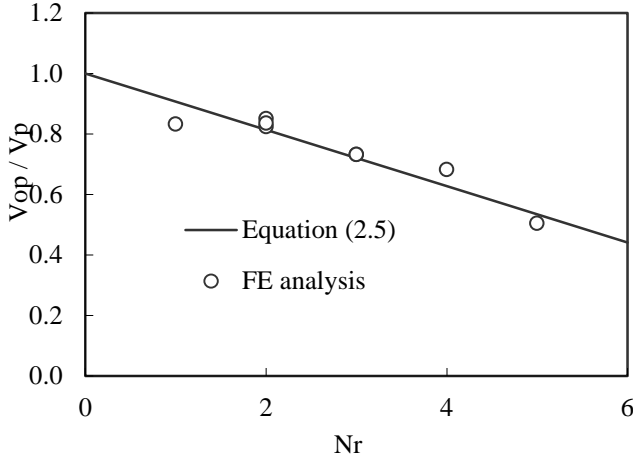


Fig. 3.4. Strength ratios of perforated infill plate to solid infill plate (aspect ratio 1.5)

4. DESIGN OF BOUNDARY COLUMNS OF PERFORATED STEEL SHEAR WALLS

As stated earlier, a simple and efficient capacity design method for design of columns of SPSWs with solid infill plates is presented in AISC Steel Design Guide 20. The method is modified here to include the effect of circular perforations in arbitrary locations. The modified design method can be summarized as follows:

- (1) For a selected perforation layout, the ratio of perforated infill plate strength to the solid infill plate strength, V_{op}/V_p , is calculated using Eq. (2.5). While determining the value of N_r to use in Eq. (2.5), it is suggested that the N_r value be rounded to the lower integer. This is a conservative approach when the boundary columns are to be designed to yield the remaining infill plates.
- (2) The distributed loads developed from yielding of the perforated infill plates can be obtained by multiplying the distributed loads developed from yielding of solid infill plates by V_{op}/V_p .

Thus, the distributed loads applied to the columns (ω_{yci} and ω_{xci}) and beams (ω_{ybi} and ω_{xbi}) and (ω_{ybi-1} and ω_{xbi-1}) at any storey i can be determined as:

$$\omega_{xci} = (V_{op}/V_p)_i R_y F_y w (\sin \alpha_i)^2 ; \omega_{yci} = (V_{op}/V_p)_i 0.5 R_y F_y w \sin 2\alpha_i \quad (4.1)$$

$$\omega_{xbi} = \omega_{xbi-1} = (V_{op}/V_p)_i 0.5 R_y F_y w \sin 2\alpha \quad (4.2)$$

$$\omega_{ybi} = \omega_{ybi-1} = (V_{op}/V_p)_i R_y F_y w (\cos \alpha)^2 \quad (4.3)$$

It is assumed that the distributed loads calculated in this way will act uniformly over the length of beams and columns in every storey.

- (4) Axial forces in the beams can be estimated using the approach outlined in AISC Steel Design Guide 20. All the beams are assumed to form a plastic hinge at their ends. With all the force components determined for the column free body diagrams, design axial forces for the columns can be easily calculated.

The detailed design method is presented elsewhere (Bhowmick 2009).

5. DESIGN EXAMPLE

One 4-storey SPSW was selected to evaluate the accuracy of the proposed design method. The 4-storey building is assumed to have the same plan area as the building considered above. For 4-storey perforated SPSWs, each shear wall is 5.7 m wide, measured from center to center of columns, with an aspect ratio of 1.5 (storey height of 3.8 m). A dead load of 4.26 kPa was used for each floor and 1.12 kPa for the roof. The live load on all floors was taken as 2.4 kPa. Design seismic loads at every storey were calculated using the equivalent static force procedure of NBCC 2005. For the 4-storey building used for this investigation, variable infill plate thicknesses were selected over the height of the SPSW, as shown in Fig. 5.1. The figure also shows the beam and column sections selected for the frame. In every storey, the top two and the bottom two perforations are located at the same distance from the beam flange closest to the perforations.

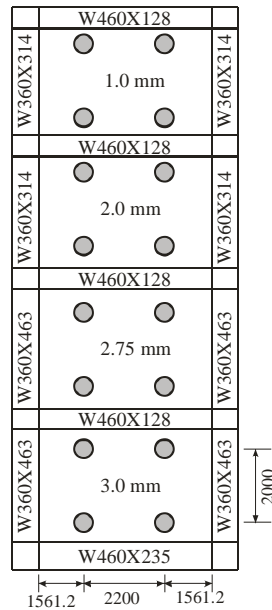


Figure 5.1. 4-storey SPSW with perforations

For the perforation pattern selected, a value of 3 was used for N_r . From Eq. (2.5), $V_{op}/V_p = 0.72$. The preliminary selection of beams and columns was based on the design loads that were obtained

after the first iteration of the proposed method with an assumed tension field inclination angle of 45° . Once preliminary sections for beams and columns were selected, the tension field angle α was calculated for every storey using the equation given in AISC 2005 and CAN/CSA-S16-01. With the revised angle of inclination, final axial forces and bending moments in the boundary columns in every storey were recalculated.

6. COMPARISON WITH SEISMIC ANALYSES

Four different seismic records were chosen for the time history response analysis. These are: (1) N-S component of the El Centro earthquake of 1940; (2) Petrolia station record from the 1992 Cape Mendocino earthquake; (3) Nahanni, Canada 1985 earthquake record; and (4) Parkfield 1966 earthquake record. The seismic records were modified using the software SYNTH (Naumoski 2001) to make them spectrum compatible for Vancouver, Canada. Nonlinear time step dynamic analyses of the 4-storey SPSW were performed using ABAQUS. The boundary conditions and material properties are the same as for the single storey SPSWs described earlier. In the finite element analyses, the storey gravity loads were represented as lumped masses on the columns at every floor. A damping ratio of 5% in Rayleigh proportional damping was selected for all the seismic analyses.

Axial forces and bending moments for the boundary columns of the 4-storey SPSW were obtained from nonlinear seismic analysis. Figure 6.1 presents the envelopes of absolute maximum column axial forces and column moments obtained from the seismic analyses. The maximum column axial force developed at the base of the 4-storey perforated SPSW from the time history analyses, 7450 kN, for the Petrolia 1992 earthquake record, is only 3.3% lower than the proposed design axial force, 7700 kN. Figure 6.1 shows that the peak seismic demand for flexure at the base of the columns, 1340 kN·m, for the Petrolia 1992 earthquake record, is 34.3% lower than the proposed design moment of 2040 kN·m.

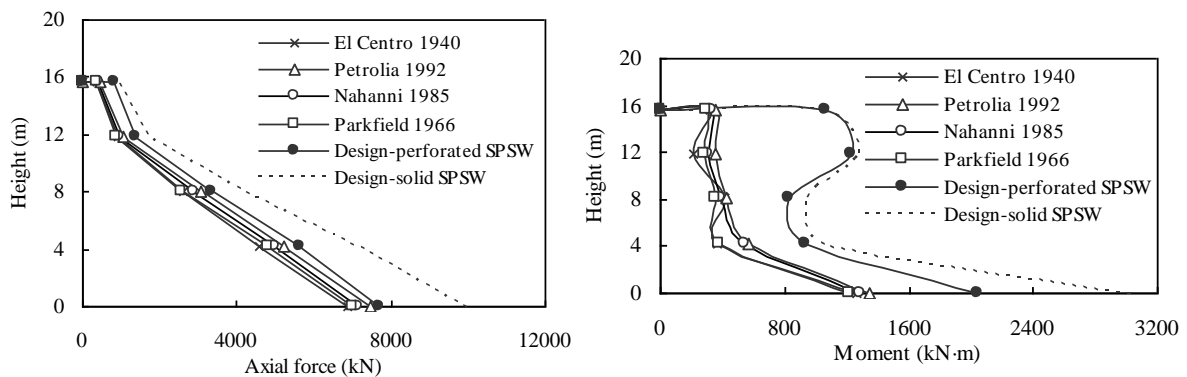


Figure 6.1. Peak column forces for 4-storey perforated SPSW

One of the objectives of introducing perforations into the infill plates was to reduce the over-strength in order to reduce the design forces for capacity design of the boundary members of the SPSWs. To demonstrate how perforations help reduce the design forces, design forces were calculated for the same 4-storey SPSW with solid infill plates, following the capacity design method presented in the AISC Steel Design Guide 20. The design forces calculated for the 4-storey SPSW with solid infill plates are compared with the design forces for the 4-storey SPSW with perforated infill plates in Fig. 6.1. Figure 6.1 shows that the design column axial forces in every storey of the perforated SPSW are lower than those for the SPSW with no perforations. The design column axial force at the base of the 4-storey perforated SPSW, 7700 kN, is 23% lower than the design axial force for the SPSW with no perforations. Also, the maximum bending moment at the base of the column of the perforated SPSW, 2040 kN·m, is 33% lower than the design moment for the SPSW with no perforations. The significant benefit of the plate weakening from the four perforations selected for each storey is evident.

7. CONCLUSIONS

A series of finite element analyses of unstiffened SPSWs with different perforation patterns was performed. The analyses show that the shear strength of an infill plate with circular perforations can be calculated by reducing the shear strength of the solid infill plate by the factor given by Eq. (2.5). The equation was found to give excellent predictions of reduced shear strengths of SPSWs with different patterns of perforations, different perforation diameters, and different infill plate aspect ratios.

A procedure for calculating the design force effects for columns of SPSWs with circular perforations in the infill plates is presented. Design column moments and axial forces from the proposed procedure were shown to agree very well with the results of nonlinear seismic analyses of 4-storey SPSW with circular perforations in the infill plates. Furthermore, the advantages of having perforations in the infill plates were demonstrated.

ACKNOWLEDGEMENTS

This work was supported by the Steel Structures Education Foundation and the Natural Sciences and Engineering Research Council of Canada. Their support is gratefully acknowledged.

REFERENCES

- AISC. (2005). Seismic provisions for structural steel buildings. American Institute of Steel Construction, Chicago, IL, USA.
- Berman, J. W., and Bruneau, M. (2005). Experimental investigation of light-gauge steel plate shear walls. *ASCE Journal of Structural Engineering* **131**:2,259-267.
- Bhowmick, A. K. (2009). Seismic analysis and design of steel plate shear walls. PhD dissertation, University of Alberta, Edmonton, AB, Canada.
- Canadian Standards Association, CAN/CSA-S16-01. (2009). Limit States Design of Steel Structures, Toronto, Ontario, Canada.
- Cortes, G., and Liu, J. (2011). Experimental evaluation of steel slit panel–frames for seismic resistance. *Journal of Constructional Steel Research* **67**:2,181-191.
- Hibbitt, Karlsson, and Sorensen. (2007). ABAQUS/Standard User's Manual. Version 6.7, HKS Inc., Pawtucket, RI, USA.
- Hitaka, T. and Matsui, C. (2003). Experimental study on steel shear walls with slits. *ASCE Journal of Structural Engineering* **129**:5,586-595.
- Naumoski, N. (2001). Program SYNTH-generation of artificial accelerogram history compatible with a target spectrum. User's manual, Dept. of Civil Engineering, University of Ottawa, Ottawa, ON, Canada.
- NBCC, National Building Code of Canada. (2005). Canadian Commission on Building and Fire Codes, National Research Council of Canada, 12th ed. Ottawa, ON, Canada.
- Purba, R. H. (2006). Design recommendations for perforated steel plate shear walls. M.Sc. Thesis, State University of New York at Buffalo, Buffalo, N.Y, USA.
- Roberts, T.M. and Sabouri-Ghomi, S. (1992). Hysteretic characteristics of unstiffened perforated steel plate shear panels. *Thin Walled Structures* **14**:139-151.
- Sabelli, R., and Bruneau, M. (2007). Steel design guide 20: steel plate shear walls. American Institute of Steel Construction, Chicago, IL, USA.
- Vian, D. (2005). Steel plate shear walls for seismic design and retrofit of building structures. PhD dissertation, State Univ. of New York at Buffalo, Buffalo, N.Y, USA.
- Xue, M. and Lu, L-W. (1994). Interaction of infilled steel shear wall panels with surrounding frame members. Proceedings, Annual Task Group Technical Session, Structural Stability Research Council, Lehigh University, Bethlehem, Pa, USA.